NB-WiFi: IEEE 802.11 and Bluetooth Low Energy combined for Efficient Support of IoT

Leif R. Wilhelmsson*, Miguel M. Lopez†, Dennis Sundman†
Ericsson Research, *Mobilvägen 1, SE-223 62 Lund, Sweden
Ericsson Research, †Torshamnsgatan 23, SE-164 40 Kista, Sweden
Email: {leif.r.wilhelmsson, miguel.m.lopez, dennis.sundman}@ericsson.com

***Abstract*—Key features of the two dominating standards for the unlicensed bands, IEEE 802.11 and Bluetooth Wireless Technology, are combined to obtain a physical layer (PHY) with several desirable features for internet of things (IoT). The proposed PHY, which is referred to as Narrow-band WiFi (NB-WiFi) can be supported by an OFDM transceiver available in an IEEE 802.11 access point (AP). In addition, NB-WiFi supports concurrent use of low data rate IoT application and high data rate broadband using IEEE 802.11ax technology, based on a single IFFT/FFT in the AP. In the sensor node, Bluetooth Low Energy (BLE) hardware can be reused, making it suitable for dual mode implementation of BLE and NB-WiFi. The performance of the proposed PHY is simulated for an AWGN channel, and it achieves about 10 dB improved sensitivity compared to a typical BLE receiver, due to the lower data rate.**

Keywords: Wi-Fi, 802.11ax, Bluetooth Low Energy, OFDMA, GFSK

I. Introduction

In this work we propose a new physical layer (PHY) based on combining key advantages of the Bluetooth Low Energy (BLE) [1], [2] and the IEEE 802.11 standards, namely the power efficiency of BLE and the wide availability of IEEE 802.11 infrastructure. We denote this PHY Narrow-Band WiFi (NB-WiFi). To enable low cost and coin cell operated IoT devices, the modulation is compliant with, although not identical to, Gaussian Frequency Shift Keying (GFSK). This allows vendors to re-use BLE chip-set designs and provides the IoT devices the possibility to operate in multiple modes; one BLE mode and one IoT mode. In order to leverage on the wide-spread availability of 802.11, NB-WiFi is made compatible with the Orthogonal Frequency Division Multiple Access (OFDMA) design of the upcoming 802.11ax standard [3],[4]. The OFDMA compatibility provides spectrum efficiency, while allowing re-use of hardware in Access Points (APs) supporting IEEE 802.11ax.

Internet of Things (IoT) is expected to vastly increase the number of connected devices. A significant share of these devices will likely operate in unlicensed bands, particularly the 2.4 GHz Industrial, Scientific, and Medical (ISM) band. IoT applications are foreseen to often have rather different requirements and features compared to conventional high data-rate home applications like file download and video streaming. Many use cases for IoT can be found in an ordinary home, and may be related to various sensors, actuators, etc. These IoT applications would typically only require low data-rates.

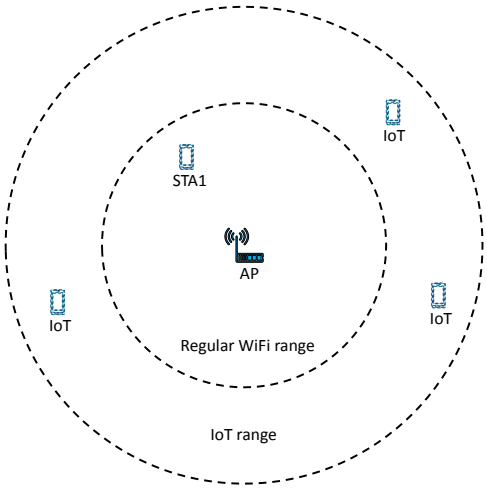

Fig. 1. Deployment where an AP support low cost IoT devices and high data rate users concurrently.

Moreover, IoT devices may be battery powered and thus power limited. They may also be located in hard to reach places like basements, requiring longer range than for example BLE. This is illustrated conceptually in Figure 1. The number of IoT devices is expected to be huge which means that although the amount of data to each device may be small, the aggregated IoT data may still be substantial. Standards that are expected to play a key role for IoT services are Bluetooth Wireless Technology, in particular BLE, and future versions of IEEE 802.11, like 802.11ax.

If IoT applications are to share the 2.4 GHz band with high data rate applications, sharing by means of time division multiplexing is not expected to be a good approach. Since the data-rate for the IoT system is low for individual links, it may be hard to obtain good spectrum efficiency by time division. Instead it is preferable if the two systems, i.e. the IoT system and the high data rate system, could operate concurrently. As concurrent operation is supported in IEEE 802.11ax by means of OFDMA, the suggested approach is to reuse the same numerology developed in IEEE 802.11ax and leverage on the OFDMA capability to achieve this.

The remaining part of the paper is organized as follows. In Section II the PHY's for BLE and 802.11ax are briefly discussed, and in particular some key PHY parameters of the

978-1-5090-4183-1/17/$31.00 ©2017 IEEE

respective air interface are introduced. Section III describes how the two air interfaces can be made compatible with one another by proper selection of some of the parameters. Simulation results for the proposed PHY are provided in Section IV, including both downlink (DL) and uplink (UL) transmissions. Finally, the conclusions are presented in Section V.

II. Background discussion of BLE and IEEE 802.11

Bluetooth originally intended to become the *de facto* standard for connecting accessories to the mobile phones [5], and the specification allows for low cost single chip implementation [6]. With the release of Bluetooth 4.0, BLE was introduced to further address the need for low power support. BLE's technical strength lies primarily in the low complexity radio [1], [2], allowing for low average power consumption and low peak power. The former being essential for battery life time, and the latter for allowing operation using coin cell batteries. To facilitate the low complexity radio, the PHY in BLE is based on GFSK [1]. Since GFSK is a constant envelope modulation, the power amplifier (PA) requires less back-off when transmitting at maximum power, resulting in increased power efficiency in the transmitter. BLE also has a substantial market presence in various consumer products.

Meanwhile, the original IEEE 802.11 standard [11] supported data rates of 1 and 2 Mb/s using single carrier modulation. With the introduction of IEEE 802.11a, a step from single carrier modulation to OFDM was taken. Later standards, such as 802.11g, 802.11n, and 802.11ac [7] are all based on OFDM targeting increasingly higher data rates. IEEE 802.11ax is an upcoming standard currently under development in the IEEE 802.11 working group, targeting high data-rate applications and efficient multi-user support. To support high data rates, IEEE 802.11ax is based on a wide band OFDMA PHY layer [4]. For IoT applications in the 2.4 GHz ISM band, IEEE 802.11 today mainly uses the rather old 802.11b standard. Although widely spread, IEEE 802.11b is not as spectrum efficient as more recent standards. For IoT applications, IEEE 802.11 has recently developed 802.11ah [8], whose PHY is based on a down-clocked version of 802.11ac [9],[7]. However, this standard is limited to sub 1 GHz bands, which are not globally harmonized. Since it is advantageous to operate in a globally available band, the NB-WiFi concept is primarily intended for operation in the 2.4 GHz band. IEEE 802.11 has a great strength in that it is the *de facto* standard used in homes for wireless high rate access. However, since the PHY layer is not designed for IoT applications, it is neither optimized for cost nor power consumption, which are features highly beneficial for IoT devices. We now list some key parameters for BLE and IEEE 802.11ax.

A. BLE - Key Parameters

The PHY for BLE uses frequency hopping, but is slightly different from classic Bluetooth in that the channels are separated by 2 MHz, rather than 1 MHz. This allows for an increase of the modulation index of the GFSK signal which improves the sensitivity in addition to making the demodulation less sensitive to frequency errors. BLE is based on binary GFSK with a symbol rate of 1 Ms/s. The bandwidth-time (BT) product is 0.5 and the modulation index h is 0.5, which results in a maximum frequency deviation of 250 kHz. Two key parameters for BLE are therefore:

- Frequency deviation of ± 250 kHz.
- Symbol duration of $T_s = 1$ μs.

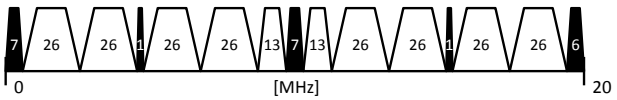

Fig. 2. Illustration of OFDMA as specified in IEEE 802.11ax. The numbers represent the amount of sub-carriers allocated for each resource unit. Unused sub-carriers are indicated with black.

B. IEEE 802.11ax - Key Parameters

Modern IEEE 802.11 systems use OFDM. The smallest supported bandwidth in the 2.4 GHz ISM band is 20 MHz, based on a 64 point FFT size with a sampling frequency of $F_s = 20$ MHz. In the development of 802.11ax, which is targeting dense deployment and also better outdoor performance [3], the FFT size is increased to 256 points for a 20 MHz channel in order to reduce the overhead caused by the cyclic prefix (CP). In addition, longer CP's are also introduced to better handle larger delay spread. To enhance the support for many high rate users, OFDMA is introduced in IEEE 802.11ax, both for DL and UL transmission. The total system bandwidth is divided into resource units (RU) of variable bandwidths. In the case of a 20 MHz channel, up to 9 users can be scheduled simultaneously using the smallest RU, which consists of 26 sub-carriers, see Figure 2.

Some key parameters for 802.11ax are [4]:

- FFT size of 256 resulting in sub-carrier spacing of $20 \text{ MHz}/256 = 78.125$ kHz.
- Duration of the useful OFDM symbol part: $T_u = 12.8\mu$s.
- CP duration of $T_{cp} = 0.8, 1.6,$ or 3.2μs.
- OFDMA capable, where the smallest RU allocation for a user is 26 sub-carriers $\simeq 2$ MHz.

III. NB-WiFi Physical Layer

We have chosen the following design goals for the NB-WiFi PHY in order to be well suited for IoT applications. The PHY shall:

1) Permit concurrent operation of NB-WiFi and high data-rate devices.
2) In the AP, support NB-WiFi at a small additional cost, where cost refers to development and hardware.
3) In the non-AP nodes, support efficient dual-mode implementation of NB-WiFi and BLE.

We have introduced Goal 1 to enable good spectral efficiency. Concurrent operation is achieved by OFDMA, allowing the possibility to allocate some RU's to the IoT system and the remaining RU's to the high data-rate system. Goal 2 is introduced to leverage on the ubiquity of IEEE 802.11. It can

TABLE I
A TABLE WITH ALTERNATIVE NUMEROLOGIES

FFT	$T_u[\mu s]$	$T_{cp}[\mu s]$	N	R_b[kb/s]	bins	bin freq. [kHz]
256	12.8	3.2	16	62.5	± 3	± 78.125
128	6.4	1.6	8	125	± 2	± 312.5
64	3.2	0.8	4	250	± 1	± 312.5
32	1.6	0.4	2	500	± 1	± 625

be realized at the AP by means of a single IFFT/FFT for both systems. Because of this, support for IoT and high data-rate devices can be provided at a small additional cost once the 802.11ax chipsets are available. Goal 3 is introduced to take advantage of the energy and cost efficient BLE chip-sets. It is realized in the non-AP node by using GFSK with the same modulation parameters as BLE.

Note that care must be taken to ensure compatibility among nodes, since OFDM is used on one side of the communication link, while GFSK is used on the other. To achieve the compatibility, the length of the CP in the OFDMA system is a key design parameter.

In order to allow for the IFFT to be used for transmission and the FFT to be used for reception, the OFDMA symbol rate much be made to match the symbol rate used by BLE. Because the duration of the FFT is determined by the IEEE 802.11 standard and the symbol rate of the GFSK signal is determined by BLE, the only parameter that can be selected is the duration of the CP. Specifically, we need to select

$$T_u + T_{cp} = NT_s, \tag{1}$$

where N is an integer, and the other parameters are defined in the previous section. It is readily seen that for 802.11ax with $T_u = 12.8\mu$s, the only choice for T_{cp} is $T_{cp} = 3.2\mu$s, which gives $N = 16$. This means that effectively $N = 16$ GFSK symbols need to be processed by the NB-WiFi receiver for every IFFT/FFT operation in the AP. In the uplink these 16 GFSK symbols are generated by means of a repetition code. The reason N is required to be an integer is that the OFDM symbol boundaries then can be made to coincide with the symbol boundaries for the GFSK symbols.

As the frequency deviation of the GFSK signal is ± 250 kHz and the sub-carrier spacing in the OFDM signal is 78.125 kHz, we select to use the sub-carriers located at ± 3 sub-carrier spacings (i.e. ± 3 FFT bins) from the center of frequency f_0 of the RU allocated to the IoT node. That is, we use the sub-carriers at $f_0 \pm 234.375$ kHz ($3 \cdot 78.125 = 234.375$).

Throughout the description above, $N = 16$ was used to ensure compatibility between BLE and IEEE 802.11ax hardware, resulting in a bit rate R_b of 62.5 kb/s. If compatibility with the IEEE 802.11ax standard is not required, alternative numerologies can be used to obtain other bit rates. Feasible alternatives with corresponding data rates are shown in Table I, where the first row corresponds to the previous discussion.

In the following we will explain the downlink and uplink procedures for the AP and non-AP (e.g. IoT) devices, respectively.

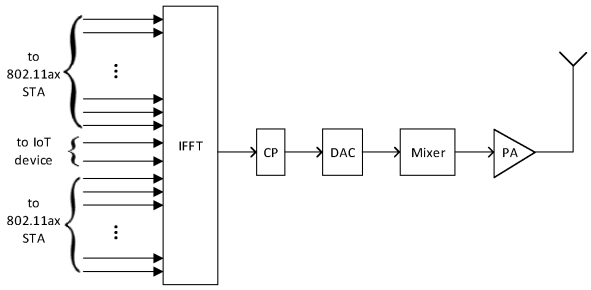

Fig. 3. Illustration of the principle for the TX processing in the DL.

A. Downlink

In the DL, the AP sends data simultaneously to IoT devices and 802.11ax stations (STA). First we explain the transmitter (i.e. AP) and then the receiver (e.g. IoT device).

In the AP, the signals intended for both the IoT device and the 802.11ax STA's are generated by a single IFFT, see the block diagram in Figure 3. In this figure the IoT data is arbitrarily located at the center of the used spectrum, whereas the signals intended for 802.11ax STA's are located on both sides of the NB-WiFi signal. The block diagram further contains a block where the CP is inserted, a digital-to-analog converter (DAC), a mixer for up-conversion to radio frequency (RF), a power amplifier (PA), and an antenna.

The signal, after the CP insertion, is illustrated in a time-frequency diagram in Figure 4. The CP is not explicitly indicated for the NB-WiFi signal to emphasize that the NB-WiFi receiver does not treat the signal as an OFDM signal and does not remove the CP. Instead the NB-WiFi receiver treats the signal segment corresponding to the CP as a useful part of the received signal, i.e., as repetition coded GFSK.

The TX spectrum of an isolated NB-WiFi signal, generated with random data, is depicted in the upper part of Figure 5. The pronounced peaks in the TX spectrum are, as expected, found with an offset of ± 234.375 kHz, which are the frequency bins in the IFFT used for the NB-WiFi signal.

In the IoT device (i.e. the receiver), we make use of a simple discriminator demodulator, that is, the signal is differentiated in the receiver. Before the signal is differentiated, it is filtered through a low-pass filter acting as a channel selective filter (CSF). As can be seen in Figure 6, the eye-opening is essentially 16μs wide and the noise margin corresponds to the 234 kHz frequency of the sub-carriers. The glitches at around 1μs and 17μs in the figure are due to discontinuities between symbols in the OFDM signal. Note that no windowing or filtering is implemented in the transmitter, which could significantly reduce the magnitude of these glitches.

B. Uplink

In the UL, an IoT device sends data to an IEEE 802.11ax AP in the RU allocated to it. This may happen concurrently with other transmission either from 802.11ax STA's, or other IoT devices in other RU's.

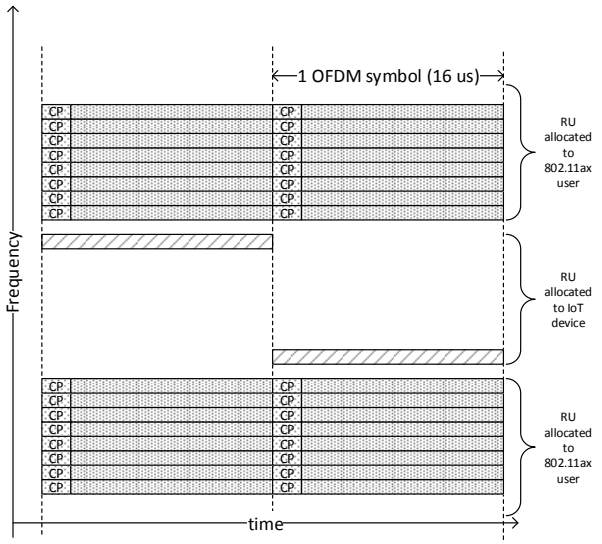

Fig. 4. Illustration of how the IoT signal is transmitted together with the 802.11ax signal.

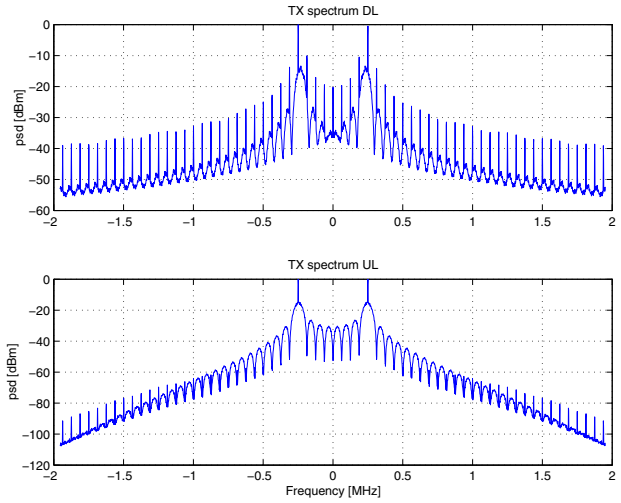

Fig. 5. TX spectra for the DL and UL.

In the AP, a single FFT is used to process both 802.11ax and the NB-WiFi signal as illustrated in Figure 7. Similar to the DL, the NB-WiFi signal is here placed in the center with 802.11ax signals on both sides. The block diagram contains an antenna, a low noise amplifier (LNA), a mixer for down-conversion, an analog-to-digital converter (ADC), a crossed block illustrating CP removal, and the FFT.

In the IoT device (i.e. the NB-WiFi transmitter), the signal is generated with a rate-$1/16$ repetition code followed by GFSK modulation using the parameters from Section II-A. The spectrum of the TX signal is depicted in the lower part of Figure 5. In this case the pronounced peaks in the spectrum are found at ± 250 kHz, and the spectrum decay is significantly better than for the DL due to the Gaussian filtering. The

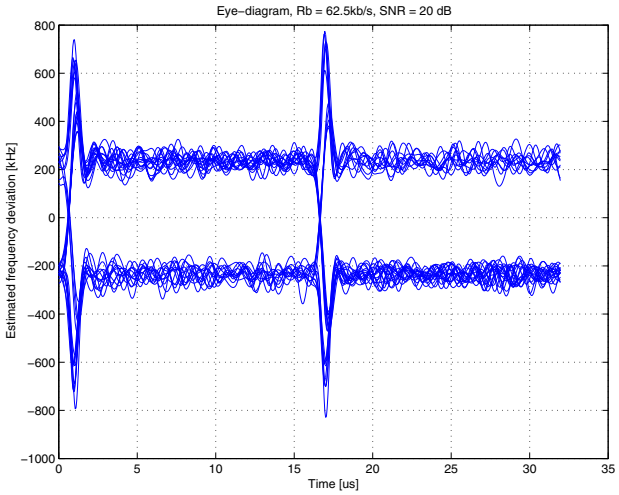

Fig. 6. Eye diagram in the IoT device, when using a discriminator type receiver. In this figure we have used a third order Butterworth low pass filter with cut-off frequency 500 kHz.

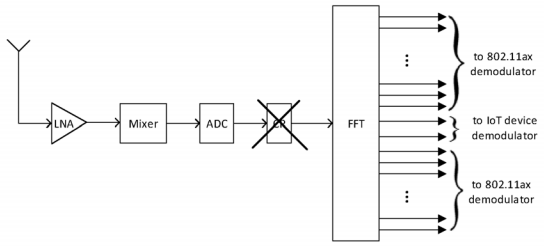

Fig. 7. Illustration of the principle for the RX processing in the UL.

receiver algorithm applied in this example uses the frequency bins corresponding to ± 234 kHz.

Figure 8 shows the instantaneous frequency deviation of the transmitted NB-WiFi signal. The dashed lines represent the GFSK impulse responses corresponding to each of the 16 individual bits in one codeword. The continuous lines represent the actual output signal, when the ISI among all the symbols is taken into account. The upper part of the figure represents a logical 1, and the lower part a logical 0. Referring to this figure, it can be seen that the repetition-coded GFSK signal is suitable to be demodulated by an FFT. The impact of the Gaussian filter is limited to less than 1 μs in the beginning and in the end of the repetition coded symbol when there are symbol transitions (i.e. when transitioning from a logical 0 to a 1, or vice versa). By synchronizing the transmitter and the receiver such that the transitions coincide with the CP of the 802.11ax signal, it will be removed prior to applying the FFT, and as a result a pure tone is input to the FFT.

IV. Simulation Results

To evaluate the performance, simulations are performed for an additive white Gaussian noise (AWGN) channel. Due to that the bandwidth of the NB-WiFi signal is similar to BLE, i.e., on the order of 1 MHz, the channel may be assumed to

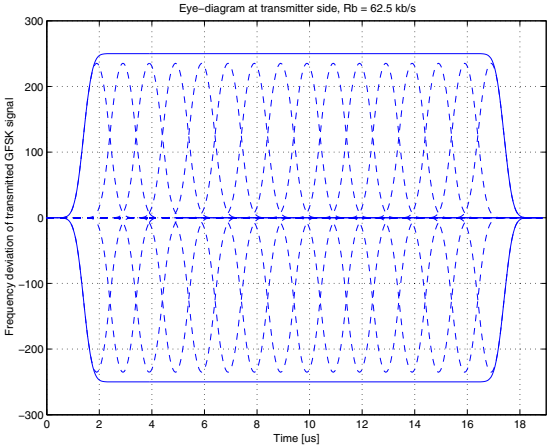

Fig. 8. This figure shows that ISI among consecutive GFSK pulses results in pure tones. In this figure we show the resulting tones for a logical 1 and a logical 0 at the same time.

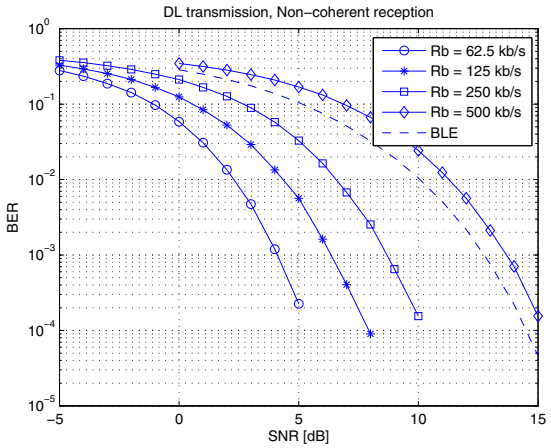

Fig. 9. BER vs SNR for non-coherent reception in the IoT device, i.e., DL.

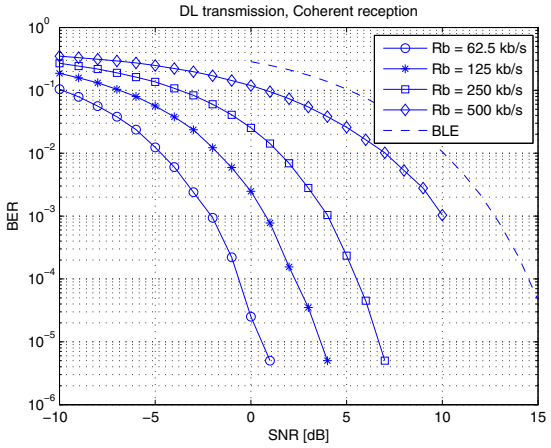

Fig. 10. BER vs SNR for coherent reception in the IoT device, i.e. DL.

be frequency non-selective for the rms delay spread expected to be experienced in typical applications [12].

Although effectively both DL and UL transmissions use a simple repetition code, the way the transmitter and receiver are implemented are fundamentally different. For the DL, soft information from N symbols are generated and combined. For the UL, the coded symbols are effectively combined by applying the FFT and the decision is based on the FFT output.

The performance plots also include results for BLE, which were obtained using a receiver based on a simple frequency discriminator and serve as a benchmark. The SNR is defined as the carrier-to-noise ratio measured over a bandwidth of 1 MHz, which is a reasonable bandwidth for a CSF used in BLE. The bit rate in BLE is 1 Mb/s, whereas the bit rates in NB-WiFi are considerably smaller to obtain better sensitivity.

A. Simulation set-up

The IoT device is simulated assuming an implementation representative for BLE with parameters as described in Section II-A and Table I. The AP is based on 802.11ax with parameters as described in Section II-B and Table I.

For the CSF in the IoT device, a third order Butterworth low pass filter with cut-off frequency 500 kHz is used. This is representative of what can be found in a typical BLE receiver. We evaluate DL and UL performance assuming both coherent and non-coherent receivers.

B. Downlink transmission

Figure 9 shows the bit error rate (BER) obtained using an OFDM transmitter (as illustrated in Figure 3) and a non-coherent receiver with a frequency discriminator, similar to what is typically used in a BLE receiver. In Figure 9, the data rate is increased in steps 62.5 kb/s, 125 kb/s, 250 kb/s, and 500 kb/s. We notice a loss of slightly less than 3 dB for each of the first two steps, and then a loss exceeding 3 dB when going to 500 kb/s. The reason why the loss is less than 3 dB for the first two steps is that the receiver operates at relatively low SNR's, where the non-linear demodulator combined with repetition coding suffers from non-coherent combining losses. The large loss in the last step, when going to 500 kb/s, is due to that the CSF is only 500 kHz wide, while the sub-carriers used are at ± 625 kHz. This means that the desired signal is somewhat attenuated by the filter.

Figure 10 shows the BER when the receiver uses coherent reception. As can be seen, the performance is significantly improved compared to the non-coherent receiver. In addition, there is an expected 3 dB loss in sensitivity when the data rate is increased by a factor of two. Similar to the previous figure, the CSF attenuates the desired signal for the highest data rate.

C. Uplink transmission

Figure 11 shows the BER when the receiver is non-coherent and the metric used in the demodulator is the amplitude at the two FFT bins closest to the corresponding frequencies ± 250 kHz sent by the NB-WiFi transmitter. We notice that the BER curves are not separated by the expected 3 dB for each doubling of the data rate. This will be explained later.

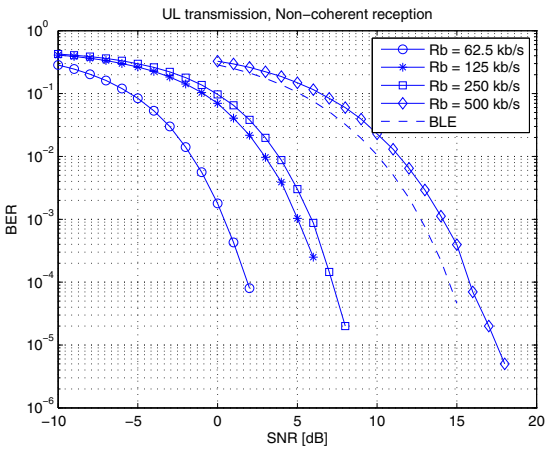

Fig. 11. BER vs SNR for non-coherent reception in the AP device, i.e. UL.

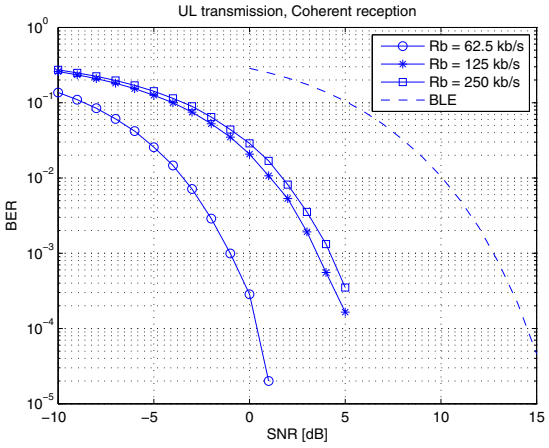

Fig. 12. BER vs SNR for coherent reception in the AP device, i.e. UL.

Figure 12 shows the BER when the receiver is coherent. After proper de-rotation (equalization) of the FFT output at the two bins, the decision is taken based on which bin has the largest real valued component. There is 1-2 dB gain using a coherent instead of a non-coherent receiver. Similar to the previous figure, the BER curves are not separated by the expected 3 dB for each doubling of the data rate.

As pointed out in the descriptions of Figure 11 and 12, the performance losses incurred when doubling the data rate are not regular. The explanation to this irregularity is the mismatch between the transmitted frequency of ± 250 kHz and the frequency of the bins used to make the bit decision, which are at ± 234 kHz. The expected loss due to frequency mismatch is

$$loss_{dB} = 20 \log_{10} \operatorname{sinc} \left(\frac{f_{mismatch}}{\Delta f} \right), \qquad (2)$$

where $\operatorname{sinc}(x) = \sin(\pi x)/(\pi x)$, $f_{mismatch}$ is the mismatch between the sent frequency and the frequency of the FFT bin, and Δf is the sub-carrier spacing. For the data rates 62.5 kb/s, 125 kb/s, and 250 kb/s, these losses become

- $N = 16 : -0.58$ dB
- $N = 8 : -2.4$ dB
- $N = 4 : -0.58$ dB

That is, the mode corresponding to 125 kb/s suffers about 1.8 dB more than the 62.5 kb/s and 250 kb/s modes, which explains why the curve corresponding to 125 kb/s is shifted about 1.8 dB to the right.

V. Conclusions

This paper introduced NB-WiFi, a PHY targeting IoT applications. The design allows low complexity implementations and provides excellent link performance. In addition it possesses two key features. First, it enables maximum reuse of hardware already available in BLE and IEEE 802.11. Second, it targets the possibility of concurrent operation with the upcoming 802.11ax standard. This ensures good coexistence with other 802.11 systems, as well as efficient spectrum use. Excellent performance was demonstrated, although reuse of hardware from BLE and IEEE 802.11ax was assumed. This shows that the proposed PHY could leverage on existing chipset designs in the development of low cost and power efficient IoT systems.

References

[1] Bluetooth, *Specification of the Bluetooth System, Core version 4.0,* 30 June, 2010, available at https://www.bluetooth.com/specifications/adopted-specifications.

[2] R. Heydon, *Bluetooth Low Energy: The Developer's Handbook*, Computer Bookshops Limited, 2012.

[3] O. Aboul-Magd, "802.11 HEW SG Proposed PAR," March, 2014, available at https://mentor.ieee.org/802.11/dcn/14/11-14-0165-01-hew-sg-proposed-par.docx.

[4] R. Stacey et al., "Proposed TGax draft specification," March, 2016, available at https://mentor.ieee.org/802.11/dcn/16/11-16-0024-01-00ax-proposed-draft-specification.docx.

[5] J. C. Haartsen, "The Bluetooth radio system," *IEEE Personal Communications,* No. 1, pp. 28-36, Feb. 2000.

[6] J. C. Haartsen and S. Mattisson "Bluetooth - A new low-power radio interface providing short-range connectivity," *Proc. of IEEE,* No. 10, pp. 1651-1661, 2000.

[7] E. Perahia and R. Stacey, *Next Generation Wireless LANs: 802.11n and 802.11ac 2nd Ed.*, Cambridge University Press, 2013.

[8] *Wi-Fi HaLow* http://www.wi-fi.org/discover-wi-fi/wi-fi-halow.

[9] IEEE 802.11, *IEEE Standard for Information Technology - Telecommunications and Information Exchange Between Systems - Local and Metropolitan Area networks - Specification Requirements. Part 11: Wireless LAN Medium Access Control (MAC) and Physical Layer (PHY) Specifications, Amendment 4: Enhancements for Very High Throughput for Operation in Bands below 6 GHz*, 2013.

[10] T. Godfrey et al., "Integrated long range low power operation for IoT," July, 2015, available at https://mentor.ieee.org/802.11/dcn/15/11-15-0775-01-wng-integrated-long-range-low-power-operation-1.pptx.

[11] G. R. Hiertz, et al., "The IEEE 802.11 Universe," *IEEE Communication Magazine,* pp. 62-70, Jan. 2010.

[12] W. H. Tranter et al. (ed), "Wireless Personal Communications - Bluetooth Tutorial and Other Technologies", Kluwer Academic Publishers, 2000.